Novel high-sensitivity coherent transceiver for optical DPSK/DQPSK signals based on heterodyne detection and electrical delay interferometer

Deming Kong (孔德明)*, Yan Li (李 岩), Xia Wu (伍 霞), Hui Wang (王 慧), Hongxiang Guo (郭宏翔), Xiaobin Hong (洪小斌), Yong Zuo (左 勇), Kun Xu (徐 坤), Wei Li (李 蔚), Jian Wu (伍 剑), and Jintong Lin (林金桐)

State Key Laboratory of Information Photonics and Optical Communications, Beijing University of Posts and Telecommunications, Beijing 100876, China

**Corresponding author: demingkong@bupt.edu.cn*

Received June 20, 2011; accepted September 5, 2011; posted online November 7, 2011

We present a novel coherent transceiver for optical differential phase-shift keying/differential quadrature phase-shift keying (DPSK/DQPSK) signals based on heterodyne detection and electrical delay interferometer. A simulation framework is provided to predict a theoretical sensitivity level for the reported scheme. High sensitivity of –45.18 dBm is achieved for 2.5-Gb/s return-to-zero (RZ)-DPSK signal, and high sensitivities of –36.83 dBm (I tributary) and –35.90 dBm (Q tributary) are observed for 2.5-GBaud/s RZ-DQPSK signal in back-to-back configuration. Transmission for both signals over 100 km is also investigated. Experimental results are discussed and analyzed.

OCIS codes: 060.1660, 060.2330.
doi: 10.3788/COL201210.030603.

Since the 1980s, numerous studies have been done on optical coherent receiver for its benefits of high receiver sensitivity, robustness to noise, and preservation of both amplitude and phase informations[1−4]. Coherent receivers can be divided into several types, including homodyne, heterodyne synchronous, and heterodyne asynchronous receivers[5,6]. Homodyne detection possesses the theoretical shot-noise-limited receiver sensitivity if the local oscillator (LO) is locked to the received signal by an optical phase-locked loop (OPLL)[7−11]. However, such a loop is complex and costly. Recently, advances in digital signal processing (DSP) enabled electrical compensation for impairments such as chromatic dispersion (CD), polarization-mode dispersion (PMD), and carrier phase error. Thus, homodyne detection with advanced modulation formats, such as quadrature amplitude modulation (QAM), i.e., 16-QAM, has become a hot spot in long-haul and high-spectrum efficiency systems[12−14]. On the other hand, heterodyne detection is much tolerable to laser linewidth and can be realized without an OPLL. Thus, this detection offers a tradeoff between sensitivity and receiver complexity. Heterodyne detection draws increasing attention in unrepeatered links such as free-space optics communications[15−17], which require high-sensitivity transceivers with less complexity. Although the in-phase (I) and quadrature (Q) noise components both affect the received signal, and the receiver sensitivity degrades compared with that of heterodyne synchronous detection, heterodyne asynchronous detection not only inherits near-shot-noise-limited performance, but is also much compact, stable, and practical than heterodyne synchronous detection, which needs an electrical carrier recovery unit.

In this letter, we propose and demonstrate a novel coherent transceiver for optical differential phase-shift keying (DPSK) and differential quadrature phase-shift keying (DQPSK) signals. The transceiver is based on heterodyne asynchronous detection and electrical delay interferometer. A passive electrical delay interferometer (EDI), which does not require phase shift control, is more stable and compact, as well as less costly compared with an optical delay interferometer (ODI) for low data rate systems. A simulation framework is first provided to predict a theoretical sensitivity level. Then by experiment, a sensitivity of –45.18 dBm (BER = 1×10^{-9}) for 2.5-Gb/s return-to-zero (RZ)-DPSK signal is achieved in back-to-back (B2B) configuration. Moreover, B2B sensitivities of –35.92 dBm (I) and –36.47 dBm (Q) for 2.5-GBaud/s RZ-DQPSK signal are achieved. Transmission performance of both signals over 100 km is investigated. Compared with the best record of DPSK receiver[18] and theoretical level[19], the present scheme achieved results that are 6 and 7 dB lower, respectively. However, since our scheme does not use any optical amplifier or any active feedback control and the requirement of laser linewidth is also released, it is therefore simple and cost-effective.

Figure 1 shows the simulation setup consisting of an optical heterodyne receiver and an EDI. Heterodyne detection down-converts the received signal into an electrical intermediate frequency (IF) signal. Theoretically, an IF of $f_{\rm IF} >> f_{\rm B}/2$ is necessary to fully recover the transmitted data[20]. The $f_{\rm B}$ is the bit rate determined optical carrier modulation bandwidth. A 10-GHz IF frequency was chosen for low-frequency noise suppression and cost effectiveness. However, we note that if the IF increases, insertion loss and the cost of electrical devices also increase. Thus, this scheme is more suitable for low data rate systems. For high data rate systems, the IF frequency should be properly decreased.

The EDI performs much like an ODI, which electrically demodulates the IF signal in a self-coherent way. The EDI has a two-tributary structure, incorporating a

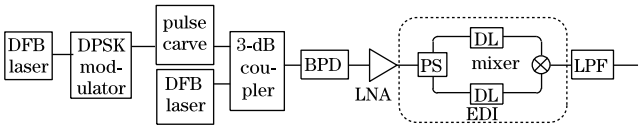

Fig. 1. Simulation setup DFB: distributed feedback; PS: phase shift.

certain delay time and a certain phase shift in each tributary. One symbol time delay is induced by one delay line (DL) corresponding to the signal envelope. On the other side, a phase shift is induced by other DL corresponding to the carrier frequency. In our scheme, one DL is set to 400 ps for 2.5-Gb/s data rate to match the IF signal envelope. The other is set to 0° for DPSK signal (corresponding to a carrier phase shift of 0°) and –12.5 ps or +12.5 ps for DQPSK signal (corresponding to a carrier phase shift of –45° and +45°).

In Fig. 1, the system data rate is 2.5 Gb/s. The signal source laser and LO laser are centered at 193.39 and 193.4 THz, respectively, which have an average power of 14 dBm. A DPSK modulator and a pulse carver are placed to generate a 50% RZ-DPSK signal. The balanced PIN photodiodes (BPD) have a 40 GHz bandwidth, 0.65 A/W responsiveness, 10 nA dark current, and 10^{-22} W/Hz thermal noise. The low-noise amplifier (LNA) has a small signal gain of 60 dB and a noise figure of 3 dB. The low-pass filter (LPF) has a 3-dB bandwidth of 0.75×2.5 GHz.

Figure 2(a) shows the simulation results for RZ-DPSK (50% duty cycle) signal. A −45.5-dBm receiver sensitivity is achieved with a 1-MHz laser linewidth. Increasing the laser linewidth to 20 MHz caused only 3-dB sensitivity penalty. This scheme is thus more tolerable to laser linewidth, providing higher stability.

Figure 2(b) shows the simulation results for RZ-DQPSK signal. A –42.5-dBm receiver sensitivity is achieved for a 1-MHz laser linewidth. A 3-dB degradation in receiver sensitivity can be expected for DQPSK signal. However, Ref. [21] predicted that for self-coherent detection, DQPSK was 6 times less tolerable than DPSK to laser frequency drift. Since our scheme incorporates two lasers, it is more sensitive to IF drift coming from unlocked heterodyne detection. The present simulation does not consider the laser frequency drift; thus, the sensitivity result is not affected by small laser linewidth values. However, larger laser linewidth values significantly affect the sensitivity result. The simulation shows a 10-MHz laser linewidth tolerance at 3-dB sensitivity penalty. The tolerance of DQPSK signal to laser linewidth is 3-dB lower than that of DPSK signal.

Figure 3 shows the experimental setup. A distributed feedback (DFB) laser, with a linewidth of approximately 1-MHz and an average power of 14-dBm, serves as the transmitter laser source. The source is then modulated through a conventional Mach-Zehnder modulator (MZM) to an optical non-return-to-zero (NRZ)-DPSK signal using an amplified electrical NRZ signal with a pattern pattern length of 2^7–1 from the pattern genrator. For NRZ-DQPSK signal, the modulation is processed through a dual-parallel MZM using two amplified electrical NRZ signals from the data out and 8 bits delayed data out of out the pattern generator, as the I and Q tributaries respectively. The NRZ PSK signals are further modulated a second MZM biased at the quadrate point to 50% RZ PSK signals by an electrically aligned 2.5-GHz sinusoidal signal. A set of 100-km TrueWave® fiber is inserted for transmission evaluation. No optical amplifier is used. The signal is then sent to an optical band-pass filter (BPF) with a 3-dB bandwidth of 0.4-nm to suppress the side modes of the laser. The average launch power of DPSK or DQPSK signal after the BPF is −4 or −12 dBm, respectively. A tunable attenuator is inserted to evaluate the sensitivity. The LO laser is a DFB laser with a line width of approximately 1-MHz and an average power of 14-dBm, which is carefully turned to be centered at 10 GHz away from the signal.

Heterodyne detection is performed with a 3-dB coupler, followed by a pair of 40-GHz BPDs with 0.65 A/W responsiveness, thus generating a 10-GHz IF signal. The power incident on the BPDs after the coupler is 11 dBm for each BPD, which mainly comes from the LO laser. Afterwards, a LNA with small a signal gain of 60 dB and

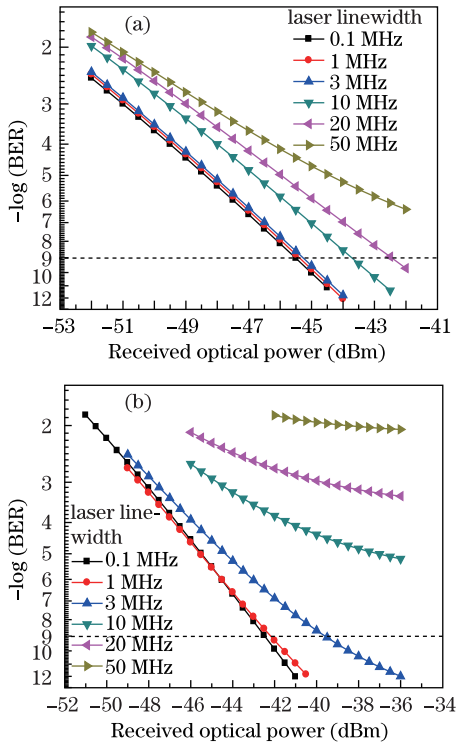

Fig. 2. Simulated BER performance of (a) 2.5-Gb/sDPSK and (b) 2.5-GBaud/s DQPSK signals under variable laser linewidth.

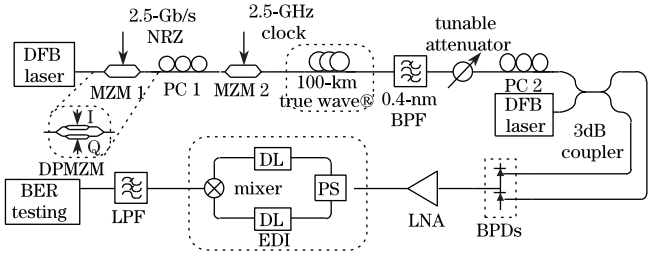

Fig. 3. Experimental setup.

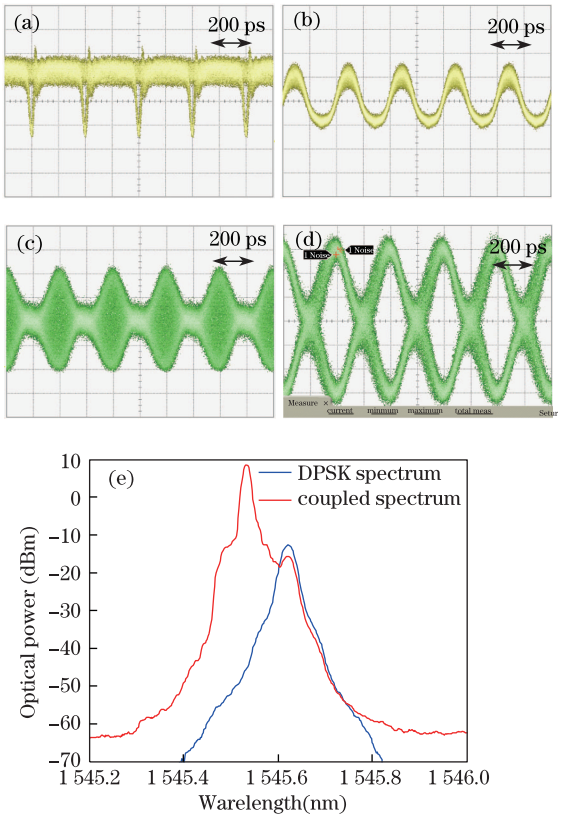

Fig. 4. Measured eye diagrams of (a) NRZ-DPSK; (b) RZ-DPSK; (c) IF signal; (d) demodulated signal; (e) measured RZ-DQPSK spectrum and coupled spectrum.

noise figure of 3-dB is applied to amplify the signal. A passive EDI consisting of a power splitter, two delay lines (plus two phase shifters), and a mixer, followed by a 2.5-GHz electrical LPF, is then used to convert the 10-GHz IF signal into baseband signal and decode the differential phase modulated signal to an amplitude modulated RZ signal. The differential decoded signal is further processed for BER testing.

Figure 4 shows the measured performance of the 2.5-Gb/s RZ-DPSK signal. Figures 4(a) and (b) show the NRZ-DPSK signal after the first MZM, and the pulse carved RZ-DPSK signal after the second MZM, respectively. Figure 4(c) shows the eye diagram of the electrical IF signal, which has a clear envelope. The demodulated baseband eye diagram after the EDI is shown in Fig. 4(d). The coupled spectrum after the 3-dB coupler of the RZ-DPSK signal and the LO shown in Fig. 4(e) indicate that the signal is 10-GHz away from the LO. Thus, the IF is 10-GHz. The time delay on two arms of EDI for demodulation of 2.5-Gb/s DPSK signal are 400 and 0 ps, respectively.

Figure 5 shows the measured performance of the 2.5-Gb/s RZ-DQPSK signal. Figures 5(a) and (b) show the eye diagrams of NRZ-DQPSK signal and RZ-DQPSK signal, respectively. The received and demodulated electrical eye diagrams for both I and Q tributaries after 100-km transmission are shown in Figs. 5(c) and (d), respectively. The spectrum of RZ-DQPSK signal and the coupled spectrum are shown in Fig. 5(e).

Figure 6 (red) shows the BER results for 2.5-Gb/s RZ-DPSK signal. Both the B2B and the 100-km transmission performances are considered, which result in sensitivities of −45.18-dBm (BER = 10^{-9}, B2B) and −44.90-dBm (BER = 10^{-9}, 100 km), respectively. A small sensitivity penalty of about 0.3-dB is observed after 100-km transmission. Compared with the simulation results, only 0.3-dB penalty is observed in B2B configuration for all system parasitics.

Figure 6 (blue) shows the BER results for 2.5-GBaud/s RZ-DQPSK signal. In the B2B configuration, sensitivities of −36.83-dBm (BER = 10^{-9}, I tributary) and −35.90 dBm (BER = 10^{-9}, Q tributary) are observed. Only the BER results from 10^{-7} to 10^{-2} could be achieved after 100-km transmission due to the insertion loss of the attenuator (approximately 4 dB). However, without the attenuator, −35.1 dBm (I tributary) and −34.52 dBm (Q tributary) optical power can be observed after 100-km transmission, with error-free performance. It is noted that the sensitivity measured in the experimental is about 5 dB lower than that in the simulation. The DQPSK signal is more sensitive to laser impairments, such as frequency drift and laser linewidth, than the DPSK signal. The main reason for this difference is the laser frequency drift, which is not considered during the simulation.

No dispersion control is applied due to the limited transmission distance and low data rate. In addition, no clear dispersion impairment is observed in the experiment. The total amount of accumulated CD after 100-km transmission is about 420 ps/nm, which is slightly larger than one unit interval (UI). However, with either a higher data rate or a longer transmission distance, dispersion

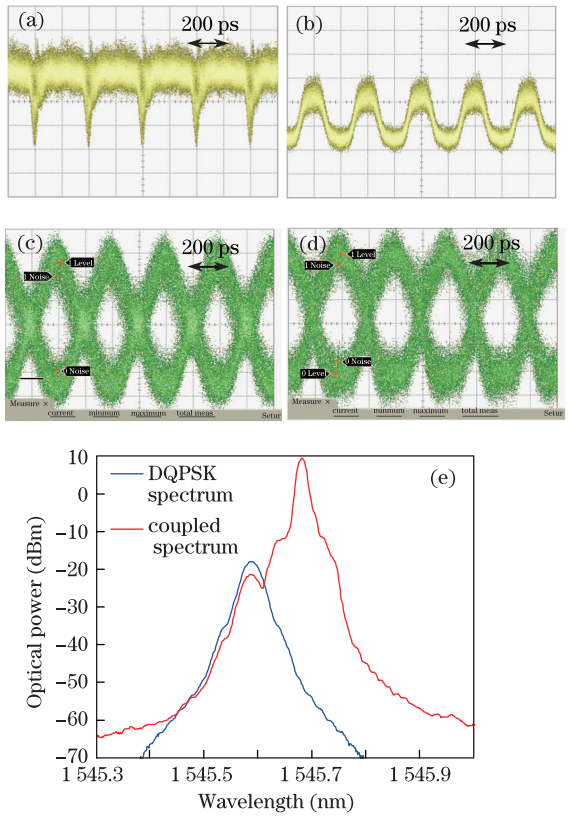

Fig. 5. Measured eye diagrams of (a) NRZ-DPSK; (b) RZ-DPSK; (c) IF signal; (d) demodulated signal; (e) measured RZ-DQPSK spectrum and coupled spectrum.

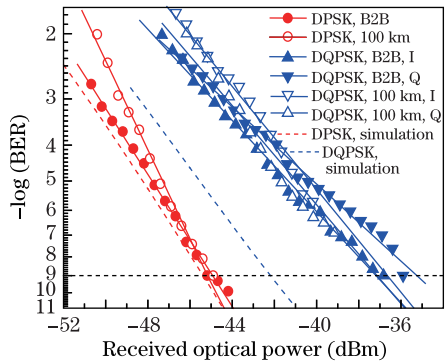

Fig. 6. (Color online) BER performance of 2.5-Gb/s DPSK and 2.5-GBaud/s DQPSK signals.

management is required due to the inter-symbol interference (ISI) induced by overlaps of adjacent pulses. The system is tolerable to a dispersion value of 2 UI.

In conclusion, we report and demonstrate a novel high-sensitivity optical coherent transceiver for DPSK and DQPSK signals based on heterodyne asynchronous detection and electrical delay interferometer. A simulation framework is provided to predict a theoretical sensitivity level. High sensitivity of −45.18 dBm is achieved for 2.5-Gb/s RZ-DPSK (50% duty cycle) signal, while high sensitivities of −36.83 and −35.90 dBm are observed for 2.5-GBaud/s RZ-DQPSK signal.

This work was supported in part by the National "973" Program of China (No. 2011CB301702), the National Natural Science Foundation of China (No. 61001121, 61006041, 60736036, and 60932004), and the Fundamental Research Funds for the Central Universities.

References

1. R. C. Steele, Electron. Lett. **19,** 69 (1983).
2. E. Ip, A. P. T. Lau, D. J. F. Barros, and J. M. Kahn, Opt. Express **16,** 753 (2008).
3. S. Chandrasekhar and X. Liu, in *Proceedings of OFC/NFOEC 2011* (2011).
4. B. Huang, N. Chi, Y. Shao, J. Zhang, J. Zhu, W. Li, and W. Liu, Chin. Opt. Lett. **8,** 856 (2010).
5. I. Lyubomirsky, IEEE Photon. Technol. Lett. **18,** 868 (2006).
6. A. H. M. R. Islam, M. Bakaul, A. Nirmalathas, and G. E. Town, IEEE Photon. Technol. Lett. **23,** 459 (2011).
7. L. G. Kazovsky, J. Lightwave Technol. **4,** 182 (1986).
8. C. Wree, D. Becker, D. Mohr, and A. Joshi, IEEE Photon. Technol. Lett. **19,** 15 (2007).
9. C. Wree, D. Becker, D. Mohr, and A. Joshi, in *Proceedings of OFC/NFOEC 2007* OMP6 (2007).
10. N. Satyan, W. Liang, A. Yariv, and G. Rakuljic, in *Proceedings of OFC/NFOEC 2009* OTuM6 (2009).
11. D. Becker, S. Datta, D. Mohr, C. Wree, S. Bhandare, and A. Joshi, in *Proceedings of OFC/NEOEC 2009* OTuG2 (2009).
12. G. Li, Adv. Opt. Photon. **1,** 279 (2009).
13. D. Ogasahara, M. Arikawa, E. L. T. de Gabory, and K. Fukuchi, in *Proceedings of OFC/NFOEC 2011* OMR3 (2011).
14. Y. Feng, H. Wen, H. Zhang, and X. Zheng, Chin. Opt. Lett. **8,** 976 (2010).
15. D. O. Caplan, M. L. Stevens, and B. S. Robinson, in *Proceedings of ECOC 2009* 9.6.1 (2009).
16. V. W. S. Chan, J. Lightwave Technol. **24,** 4750 (2006).
17. S. A. Hamilton, R. S. Bondurant, D. M. Boroson, J. W. Burnside, D. O. Caplan, E. A. Dauler, A. S. Fletcher, S. Michael, R. J. Murphy, B. S. Robinson, J. J. Scozzafava, N. W. Spellmeyer, T. G. Ulmer, and F. G. Walther, in *Proceedings of OFC/NFOEC 2011* OWX2 (2011).
18. D. O. Caplan, M. L. Stevens, J. J. Carney, and R. J. Murphy, in *Proceedings of CLEO/QELS 2006* CFH5 (2006).
19. P. A. Humblet and M. Azizoglu, J. Lightwave Technol. **9,** 1576 (1991).
20. G. P. Agrawal, *Nonlinear Fiber Optics* (Acdamic Press, San Diego, 2001).
21. H. Kim and P. J. Winzer, J. Lightwave Technol. **21,** 1887 (2003).